

Measurements of Interaction Cross Sections and Nuclear Radii in the Light p -Shell Region

I. Tanihata,^(a) H. Hamagaki, O. Hashimoto, Y. Shida, and N. Yoshikawa

Institute for Nuclear Study, University of Tokyo, Tanashi, Tokyo 188, Japan

K. Sugimoto,^(b) O. Yamakawa, and T. Kobayashi

Nuclear Science Division, Lawrence Berkeley Laboratory, University of California, Berkeley, California 94720

and

N. Takahashi

College of General Education, Osaka University, Toyonaka, Osaka 560, Japan

(Received 11 July 1985; revised manuscript received 17 September 1985)

Interaction cross sections (σ_I) for all known Li isotopes (${}^6\text{Li}$ – ${}^{11}\text{Li}$) and ${}^7\text{Be}$, ${}^9\text{Be}$, and ${}^{10}\text{Be}$ on targets Be, C, and Al have been measured at 790 MeV/nucleon. Root mean square radii of these isotopes as well as He isotopes have been deduced from the σ_I by a Glauber-type calculation. Appreciable differences of radii among isobars (${}^6\text{He}$ – ${}^6\text{Li}$, ${}^8\text{He}$ – ${}^8\text{Li}$, and ${}^9\text{Li}$ – ${}^9\text{Be}$) have been observed for the first time. The nucleus ${}^{11}\text{Li}$ showed a remarkably large radius suggesting a large deformation or a long tail in the matter distribution.

PACS numbers: 25.70.–z, 21.10.Gv, 27.20.+n

Recently, exotic-isotope beams, produced through the projectile-fragmentation process in high-energy heavy-ion reactions, were used to measure the interaction cross sections (σ_I) for all the known He isotopes.¹ This novel technique of using exotic nuclear beams makes it possible to study systematically properties of unstable nuclei. In the present paper, we report the σ_I for all the known Li isotopes (${}^6\text{Li}$, ${}^7\text{Li}$, ${}^8\text{Li}$, ${}^9\text{Li}$, and ${}^{11}\text{Li}$) and ${}^7\text{Be}$, ${}^9\text{Be}$, and ${}^{10}\text{Be}$ on the target nuclei Be, C, and Al at 790 MeV/nucleon. A firm basis has been empirically established by use of a Glauber-type calculation to extract root mean square (rms) nuclear radii from the σ_I .

The Li isotopes, except ${}^{11}\text{Li}$, and the Be isotopes were produced as secondary beams through projectile fragmentation of the 800-MeV/nucleon ${}^{11}\text{B}$ accelerated by the Bevalac at the Lawrence Berkeley Laboratory. The beam of ${}^{11}\text{Li}$ was produced from a ${}^{20}\text{Ne}$ primary beam. The isotopes produced in a production target of Be were separated by rigidity with the beam-line magnet system as described in previous papers.^{1,2} The rigidity-separated isotopes were further identified before incidence on a reaction target by velocity [time-of-flight (TOF)] and by charge (pulse height in scintillation counters). No contamination more than 10^{-3} was observed in any selected isotope beam.

The interaction cross section (σ_I) was measured by a transmission experiment using the large-acceptance spectrometer as in the measurement of the He isotopes.¹ Here σ_I is defined as the total reaction cross section for the change of proton and/or neutron number in the incident nucleus. The obtained σ_I are listed in Table I. The largest systematic error on σ_I , up to about 0.3%, came from uncertainties in the estimation of the scattering-out probability of the nonin-

teracting nuclei. All other systematic errors were estimated to be less than 0.2% of σ_I .

The interaction nuclear radius R_I is defined as

$$\sigma_I(p, t) = \pi [R_I(p) + R_I(t)]^2, \quad (1)$$

where $R_I(p)$ is the projectile radius and $R_I(t)$ is the target radius. The separability of projectile and target radii assumed in the equation was examined by use of σ_I of various projectile-target combinations. Figure 1 shows R_I of Li and Be isotopes obtained from different targets. Here the absolute scale of the radius was determined from a least-squares fitting of σ_I of ${}^4\text{He} + {}^4\text{He}$, ${}^9\text{Be} + {}^9\text{Be}$, ${}^{12}\text{C} + {}^{12}\text{C}$, ${}^4\text{He} + {}^{12}\text{C}$, and ${}^9\text{Be} + {}^{12}\text{C}$ reactions.^{1,3,4} It is seen that a projectile radius is in fact independent of target variation. As a result the assumption of the separability of projectile and target radii was demonstrated to be valid within ± 0.02 fm. This separability indicates that R_I is experimentally a well-defined size parameter of a nucleus.

TABLE I. Interaction cross sections (σ_I) in millibarns.

Beam	Target		
	Be	C	Al
${}^6\text{Li}$	651 ± 6	688 ± 10	1010 ± 11
${}^7\text{Li}$	686 ± 4	736 ± 6	1071 ± 7
${}^8\text{Li}$	727 ± 6	768 ± 9	1147 ± 14
${}^9\text{Li}$	739 ± 5	796 ± 6	1135 ± 7
${}^{11}\text{Li}$		1040 ± 60	
${}^7\text{Be}$	682 ± 6	738 ± 9	1050 ± 17
${}^9\text{Be}$	755 ± 6	806 ± 9	1174 ± 11
${}^{10}\text{Be}$	755 ± 7	813 ± 10	1153 ± 16

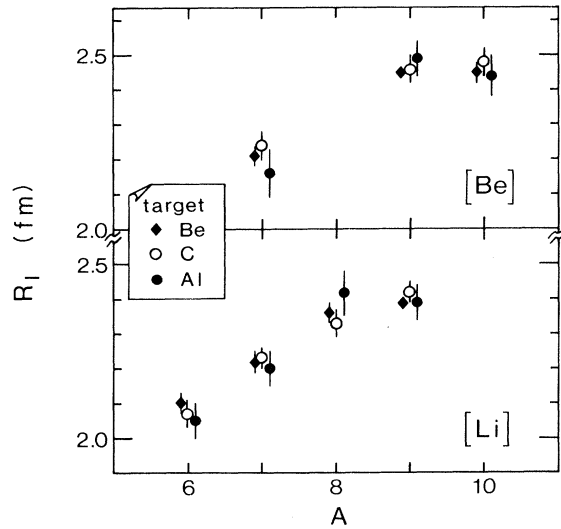


FIG. 1. R_I for Li and Be isotopes. The values obtained by three different targets agree with each other showing the separability of projectile and target R_I .

Average values of R_I deduced from the Be, C, and Al targets are, therefore, used for further discussion.

In Table II the obtained R_I (column 1) are listed together with the rms radii R_{rms}^e of the charge distribution determined by electron-scattering experiments⁵ (column 2). The dependence of R_I on the mass number (A) and that of R_{rms}^e show a noticeable difference, i.e., R_I increases with A , whereas R_{rms}^e stays almost constant for $A \geq 6$. We will now show that the difference is due to the definitions of the two radii but not due to a difference between the charge and the

matter distributions.

We relate σ_I to the rms radius by a Glauber-type calculation using Karol's prescription⁶ and show that the rms radius of nuclear-matter distribution can be determined independently of assumed model density functions. To examine the functional dependence, we employed three types of nuclear density distributions: a Gaussian,⁶ a shell-model harmonic oscillator,⁷ and a droplet model⁸ with a Yukawa folding function $[(1/r)e^{-r/b}]$. The Gaussian and the harmonic-oscillator distributions each have only one size parameter, a_G and a_{HO} , respectively. On the other hand, the droplet-model distribution has two parameters: a size parameter r_0 and a diffuseness parameter b . First, we discuss the rms radii using the Gaussian and the harmonic-oscillator distributions.

In a Glauber-type calculation nucleon-nucleon (NN) cross sections have to be given. The free NN cross sections are inappropriate, however, because the effective values may differ from the free-nucleon values because of nuclear-matter effects. In fact, it has been reported that the mean free path of the 800-MeV protons inside the nuclear matter is longer than expected from the free NN cross sections⁹ and also that the effective values of NN cross sections are smaller in uranium reactions at 900 MeV/nucleon.¹⁰ To determine the effective values of NN cross sections for the present analysis, the calculations were first made for collisions of identical stable isotopes,¹¹ i.e., ${}^4\text{He} + {}^4\text{He}$, ${}^6\text{Li} + {}^6\text{Li}$, ${}^7\text{Li} + {}^7\text{Li}$, ${}^9\text{Be} + {}^9\text{Be}$, and ${}^{12}\text{C} + {}^{12}\text{C}$. The size parameter a_G (or a_{HO}) and a scaling factor of NN cross sections were taken as parameters in order to fit the R_{rms}^e and σ_I simultaneously.

It was found that effective values of the NN cross

TABLE II. Interaction nuclear radii and rms radii, in fermis.

	R_I	e scat. R_{rms}^e	Gaussian R_{rms}^G	Harmonic oscillator		
				R_{rms}^m ^a	R_{rms}^c ^a	R_{rms}^n ^a
${}^4\text{He}$	1.41 ± 0.03	1.67 ± 0.01	1.72 ± 0.06	1.72 ± 0.06	1.72 ± 0.06	1.72 ± 0.06
${}^6\text{He}$	2.18 ± 0.02		2.75 ± 0.04	2.73 ± 0.04	2.46 ± 0.04	2.87 ± 0.04
${}^8\text{He}$	2.48 ± 0.03		2.70 ± 0.03	2.69 ± 0.03	2.33 ± 0.03	2.81 ± 0.03
${}^6\text{Li}$	2.09 ± 0.02	2.56 ± 0.10	2.54 ± 0.03	2.54 ± 0.03	2.54 ± 0.03	2.54 ± 0.03
${}^7\text{Li}$	2.23 ± 0.02	2.41 ± 0.10	2.50 ± 0.03	2.50 ± 0.03	2.43 ± 0.03	2.54 ± 0.03
${}^8\text{Li}$	2.36 ± 0.02		2.51 ± 0.03	2.51 ± 0.03	2.41 ± 0.03	2.57 ± 0.03
${}^9\text{Li}$	2.41 ± 0.02		2.43 ± 0.02	2.43 ± 0.02	2.30 ± 0.02	2.50 ± 0.02
${}^{11}\text{Li}$	3.14 ± 0.16		3.27 ± 0.24	3.27 ± 0.24	3.03 ± 0.24	3.36 ± 0.24
${}^7\text{Be}$	2.22 ± 0.02		2.48 ± 0.03	2.48 ± 0.03	2.52 ± 0.03	2.41 ± 0.03
${}^9\text{Be}$	2.45 ± 0.01	2.52 ± 0.01	2.49 ± 0.01	2.50 ± 0.01	2.47 ± 0.01	2.53 ± 0.01
${}^{10}\text{Be}$	2.46 ± 0.03		2.38 ± 0.02	2.39 ± 0.02	2.34 ± 0.02	2.43 ± 0.02
${}^{12}\text{C}$	2.61 ± 0.02	2.45 ± 0.01	2.40 ± 0.02	2.43 ± 0.02	2.43 ± 0.02	2.43 ± 0.02

^aSuperscripts m , c , and n indicate the nuclear matter, the charge, and the neutron matter distributions, respectively.

sections, 80% of the free-nucleon values, gave a good fit in the present mass range. In Fig. 2, the rms radii R_{rms}^G obtained after fitting the σ_I by use of the Gaussian distribution with effective NN cross sections are shown by the dashed line. The solid line in the figure indicates the charge rms radii R_{rms}^c obtained in the same way by use of the harmonic-oscillator distribution. It is seen that the R_{rms}^e are well reproduced with the fixed scaling factor for NN cross sections. Even the difference between the R_{rms}^e of ${}^6\text{Li}$ and ${}^7\text{Li}$ is reproduced by the harmonic-oscillator distribution because of the occupation-number difference between protons and neutrons.

This calculation also showed that R_I represents the radius where the matter density is about 0.05 fm^{-3} for $A \geq 6$ nuclei. Now it can be understood why R_I and the rms radius behave differently with increase of A : While the rms radius stays constant, the absolute density increases with A . Therefore R_I , which represents constant density, increases with A .

Having established that the rms radii of stable nuclei derived from σ_I agree with R_{rms}^e , we now extend the calculations to unstable nuclei using the effective NN cross sections. Column 4 in Table II shows the deduced R_{rms}^G and columns 5–7 show rms radii deduced by use of the harmonic-oscillator distribution (R_{rms}^m , matter radius; R_{rms}^c , charge radius; and R_{rms}^n , neutron matter radius). The R_{rms}^G and R_{rms}^m agree well for each nucleus.

Calculations using the droplet model gave further evidence that different distributions can give essentially the same values for rms radii. In this model we have two parameters, a size parameter (r_0) and a diffuseness parameter (b). It is found that a set of values of r_0 and b which fit a σ_I gives essentially same R_{rms}^m values. The R_{rms}^m were calculated with use of values¹²

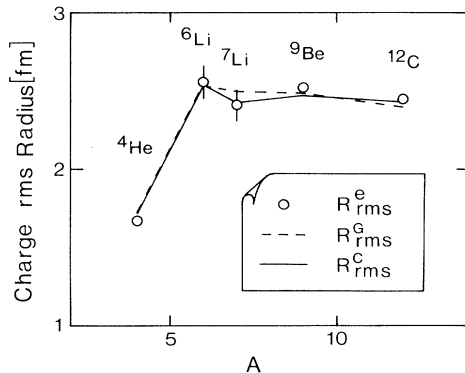


FIG. 2. Charge rms radii. Circles indicate the radii R_{rms}^e determined by electron-scattering experiments. The dashed line shows the result obtained by fitting the σ_I by a Glauber-type calculation employing a Gaussian density distribution. The solid line shows the result obtained by use of a shell-model harmonic-oscillator distribution.

of b from 0.4 to 0.8 fm for ${}^4\text{He}$, ${}^6\text{Li}$, ${}^9\text{Be}$, and ${}^{12}\text{C}$ and were found to be equal within 0.04 fm to those obtained from the harmonic oscillator.

From the preceding discussion we conclude that the nuclear matter radii deduced from σ_I are insensitive to the selection of the model density distribution. Figure 3 shows the R_{rms}^m determined by use of the harmonic-oscillator distribution. Appreciable differences of radii are observed, for the first time, between pairs of isobars with different isospin, ${}^6\text{He}$ - ${}^6\text{Li}$, ${}^8\text{He}$ - ${}^8\text{Li}$, and ${}^9\text{Li}$ - ${}^9\text{Be}$. The larger radii of the neutron-rich isotopes ${}^6\text{He}$ and ${}^8\text{He}$, which have only two protons, suggest the existence of thick neutron skins as seen in differences between R_{rms}^c and R_{rms}^n in Table II. On the other hand, a pair of mirror nuclei ${}^7\text{Li}$ - ${}^7\text{Be}$ show the same matter radius.

It is interesting to note that the nucleus ${}^{11}\text{Li}$, with the neutron number of p -shell closure in the naive shell model, shows a considerably larger radius than neighboring nuclei. It suggests the existence of a large deformation and/or of a long tail in the matter distribution due to the weakly bound nucleons. A weakly bound nucleon may enhance σ_I because it could be kicked out from the nucleus with a small momentum transfer. A rough estimation based on the energy distribution of nucleons after a nucleon-nucleon collision, however, showed that the change in separation energy from 10 MeV to zero affects σ_I by only about 3%. This binding effect, therefore, cannot explain the bulk of the observed deviation.

In summary, we have measured the interaction cross sections σ_I of nucleus-nucleus collisions using secondary beams of unstable and stable Li and Be isotopes.

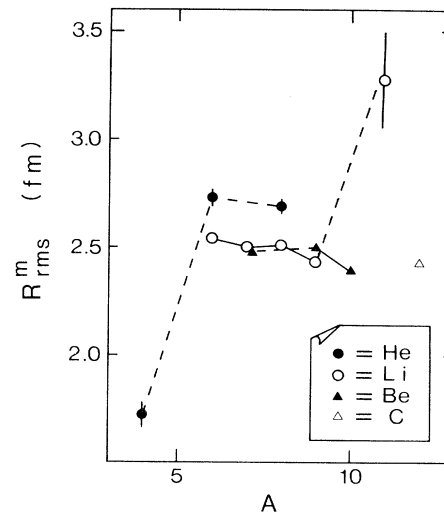


FIG. 3. Matter rms radius R_{rms}^m . Lines connecting isotopes are only guides for the eye. Differences in radii are seen for isobars with $A = 6, 8, \text{ and } 9$. The ${}^{11}\text{Li}$ isotope has a much larger radius than other nuclei.

The interaction radii R_I of these nuclei have been determined from the σ_I . The separability of R_I observed between projectile and target indicated that R_I represents a well-defined size parameter of a nucleus. The matter rms radii were deduced by use of three model density distributions: the Gaussian, the shell-model harmonic oscillator, and the droplet model. As a result, the three distributions gave essentially the same rms radii. These rms radii for stable nuclei have been found to agree well with those from electron-scattering experiments. It has been found that ^{11}Li has a radius much larger than other neighboring nuclei presented here. It suggests the existence of a large deformation and/or a long tail in the matter distribution in ^{11}Li . The differences between the matter rms radii R_{rms}^m for isobars of different isospins, ^6He - ^6Li , ^8He - ^8Li , ^9Li - ^9Be , have been observed for the first time. A pair of mirror nuclei ^7Li - ^7Be have been found to have equal R_{rms}^m .

We would like to thank Y. Matsuyama, T. Fujino, and F. S. Bieser for their technical assistance. Discussions with Dr. D. E. Greiner and Dr. W. D. Myers are gratefully acknowledged. This work was supported by the Director, Division of Nuclear Physics of the Office of High-Energy and Nuclear Physics of the U.S. Department of Energy under Contract No. DE-AC03-76SF00098, by the INS-LBL Collaboration Program, and by the Japan-U.S. Joint Program for High-Energy Physics. One of the authors (I.T.) gratefully ac-

knowledges the support of Yamada Science Foundation.

(a)Also at Lawrence Berkeley Laboratory, University of California, Berkeley, Cal. 94720.

(b)Permanent address: Faculty of Science, Osaka University, Osaka 560, Japan.

¹I. Tanihata *et al.*, Phys. Lett. **160B**, 380 (1985).

²I. Tanihata, Hyperfine Interact. **21**, 251 (1985).

³J. Jaros *et al.*, Phys. Rev. C **18**, 2273 (1978).

⁴H. H. Heckmann *et al.*, Phys. Rev. C **17**, 1735 (1978).

⁵R. C. Barrett and D. F. Jackson, *Nuclear Sizes and Structure* (Clarendon, Oxford, 1977), p. 146.

⁶P. J. Karol, Phys. Rev. C **11**, 1203 (1975).

⁷L. R. B. Elton, *Nuclear Sizes* (Oxford Univ. Press, London, 1961), pp. 21-22.

⁸W. D. Myers and K.-H. Schmidt, Nucl. Phys. **A410**, 61 (1983).

⁹I. Tanihata, S. Nagamiya, S. Schnetzer, and H. Steiner, Phys. Lett. **100B**, 121 (1981).

¹⁰D. E. Greiner *et al.*, Phys. Rev. C **31**, 416 (1985).

¹¹Here $\sigma_I(^6\text{Li}, ^6\text{Li})$ and $\sigma_I(^7\text{Li}, ^7\text{Li})$ were not directly measured but calculated from $R_I(^6\text{Li})$ and $R_I(^7\text{Li})$ by use of Eq. (1). These values were estimated to be reliable within a few percent with use of the projectile-target separability as discussed in the text.

¹²The commonly accepted value of b is ≈ 0.7 for an $A > 10$ stable nucleus and ≈ 0.4 for ^4He . J. Friedrich and N. Voegler, Nucl. Phys. **A373**, 192 (1982).